

Local Spectrum Analysis of Hybrid RANS/LES Data Using Dynamic Mode Decomposition for a Body-Wing-Tail Airframe

Erdem Dikbaş

Aerodynamics and Engineering Analysis Dept., Roketsan Inc., Elmadağ, Ankara, 06780, Türkiye

Keywords: Dynamic Mode Decomposition, Scale Resolving Simulation, External Aerodynamics, Vortex Interactions, Transient Flow, Compressible Flow

Abstract. Turbulent flow structures over an outer mould line of an external airframe, namely LK6E2, were resolved using Delayed Detached Eddy Simulation (DDES). The test case represents a compressible external flow problem with strong and involved vortex-vortex, vortex-shock, and vortex-surface interactions. The interaction between body wake vortices and the wing surfaces induces significant oscillations in the integrated aerodynamic loads of the airframe. Resonant frequencies on the integrated quantities obtained by Fast Fourier Transform (FFT) showed a strong dependency on flow incidence angle. Between 13 and 18 degrees of incidence, there is a steep change in the dominant frequency. In this study, we investigate the shift in the frequency mode and how this relates to the oscillatory behaviour of flow structures by local spectrum analysis. The study aims to understand the dynamic effects of the flow structures emerging from the different parts of the airframe. We used the Dynamic Mode Decomposition (DMD) method through the PyDMD library to process spatiotemporal data generated with DDES analysis. We reconstruct the surface pressure fields to extract coherent structures and determine associated mode shapes. Dominant modes determined by integral/FFT and local/DMD analyses agree well; thus, DMD captures the mode shift, which depends on the flow incidence angle. In the end, we are able to visualize mode shapes and have a better understanding of transient vortex interactions over the LK6E2 airframe.

1. Introduction

Body-wing-tail airframes (e.g., missiles) are occasionally exposed to vortex-surface interactions in high manoeuvre conditions. Exploration towards their mechanisms and possible consequences has been a research topic for many decades. The scientific interest in this field remains among aerospace communities due to opportunities for more detailed investigations using modern computational technologies and methods. For instance, the NATO Science and Technology Organization (STO) Applied Vehicle Technology (AVT) panel established a Task Group identified as AVT-316 (Vortex Interaction Effects Relevant to Military Air Vehicle Performance) [1]. LK6E2 was one of the research test cases developed to investigate vortex interactions on highly maneuverable transonic missiles. Hybrid RANS/LES methods were prominently employed by diverse contributors to understand the flow field around this airframe. The major findings of this collaborative research were published during special sessions at the AIAA 2022 SciTech and 2024 Aviation Conferences [2, 3]. The hybrid RANS/LES analyses provided strong insight about the unsteady flow features; though, there are still open questions remaining about spectral content of the flow structures and its effect on the overall aerodynamic behaviour of the airframe.

The LK6E2 is an external aerodynamics test case that gained its significance after extensive wind tunnel tests carried out in German-Dutch Wind tunnels (DNW) [4]. At flight Mach number of 0.85 and roll angle of 45°, rolling moment coefficient (C_l) of LK6E2 showed a significant nonlinearity between 16-18 degrees of incidence angle. During the NATO STO study [1] and subsequent studies [3, 5], strong challenges were confronted in predicting this behaviour using CFD. Practically speaking, failure in the prediction of the rolling moment during the design and analysis stage may lead to severe consequences later in flight testing and commissioning stages in terms of stability and control of a missile. Thus, we aim to improve our understanding of flow characteristics over such a configuration.

Data-driven approaches have gained popularity among fluid flow applications in recent years. Due to advancements in computer technologies, practitioners have started developing and using more involved

mathematical models; hence, amounts of flow field data have increased. Interpretation of complex flow data mostly necessitates the application of modern machine learning methods. Reduced Order Modelling (ROM) has been a powerful approach for modelling unsteady aerodynamic data [6]. Kou and Zhang [7] and Long et al. [8] provided comprehensive reviews for the use of ROM in aerospace applications with a historical perspective. According to those, two popular ROM techniques employed frequently in fluid dynamics are Proper Orthogonal Decomposition (POD) and Dynamic Mode Decomposition (DMD). Since the latter is inherently designed for the dynamic evolution of linear systems and decomposes data into modes that evolve according to their own frequency and growth rates, it is comparatively suitable for turbulence and vortex dynamics research. For this reason, we adopt the DMD technique for the analysis of unsteady flow data in the current study.

There exist several research studies about the coupling of the DMD modelling with the transient CFD simulations. Quite successful representations could be obtained for low-frequency data from two-dimensional simplistic flow problems [9, 10]. For three-dimensional realistic aerodynamic flows, the past work includes very low-speed applications, where there are no wave interactions [11, 12]. In general, DMD reconstructions on realistic flows performed weaker than on simplistic cases. Ma and Yin [13] studied an external flow over a slender body to explore the unsteady flow characteristics in the Strouhal number ($Sr = fD/U_\infty$) less than 0.3.

The current study describes an initial attempt to investigate high-frequency oscillations due to transonic flow over a missile configuration using DMD. First, we conducted a DDES analysis for different external conditions of LK6E2, as described in Ref. [3]. We collected time-dependent integrated aerodynamic coefficients and surface pressure distributions. Afterwards, we applied Fast Fourier Transform (FFT) for the integrated coefficients and DMD for the pressure distributions. In the end, generated data provided better insight into the unsteady character of complex flow interactions occurring in this test case.

2. Problem definition

The LK6E2 is a wing-body-tail configuration with a spherical nose and boattail. Its geometric details are illustrated in Figure 1. The diameter of the fuselage (D) is 50 mm, and this quantity is used as a reference length where necessary. The wing and fin sets are aligned to each other. The illustration depicts the view for the roll orientation 45°, at which all analyses in the current study are performed. The aerodynamic rolling moment, which is the main integrated quantity examined in the current study, is defined as the moment component on the axis of the fuselage (x -axis). The incidence angle (σ) is defined as the angle between the velocity direction and the x -axis. For the positive incidences, wing/fin #1 and #3 are located in windward and leeward positions, respectively.

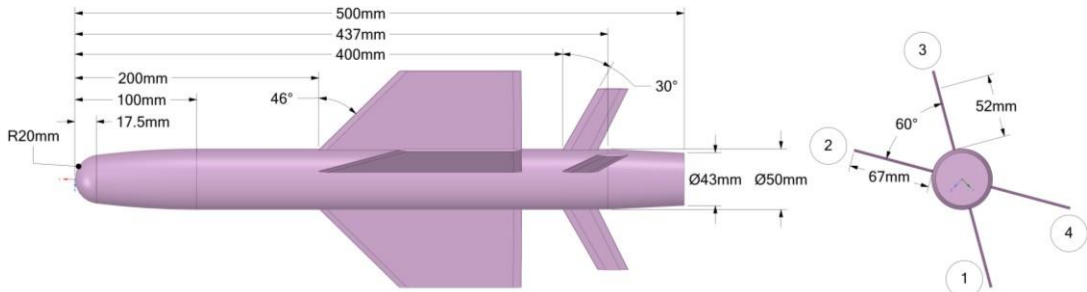


Figure 1. LK6E2 geometry, dimensions, and wing/fin numbering convention

The computations were performed with external flow speed described by Mach number of 0.85 and Reynolds number (based on D) of 500k. The flow incidence angle is variable from 10 to 18 degrees. The current study makes use of *common fine mesh* generated during the NATO STO study. The STO report [1] presents a good overview of the properties of the computational mesh.

3. Adopted models and tools

3.1. Flow analysis tools

In the current study, we utilized the open-source CFD solver *flowPsi*, which is a cell-based finite volume solver developed by Luke [14]. This code contains viscous and inviscid solvers for steady or unsteady compressible Navier-Stokes equations. The solver has been maintained as an open-source software under GPL license [15]. The computations in the current study are based on version 1.0-p4. The *flowPsi* code involves several numerical methods and models specialized for compressible flow computations. The solver accepts unstructured meshes with various types of element topology coexisting, as it has a cell-centered formulation.

The external flow analysis over LK6E2 required high-fidelity methods to resolve complex flow phenomena such as vortex and shock interactions. Thus, we decided to take advantage of scale-resolving turbulence models to capture unsteady flow characteristics with high resolution. The turbulence model used in this study is the Spalart-Allmaras (SA) model [16] combined with the Delayed Detached Eddy Simulation (DDES) approach [17].

3.2. Spectral mode decomposition tools

The spectral content was first calculated using the integrated aerodynamic coefficient data, which are time signals containing highly fluctuating data. FFT technique [18] was employed to determine the dominant frequencies.

DMD is the major method used to extract local spectral characteristics of the unsteady flow data. For the application of DMD, surface pressure data collected from the DDES were mapped into structured frames, each representing the pressure distribution at a discrete time step. Spatiotemporal data were then fed into the DMD processor in the PyDMD library [19]. This library was developed and integrated into the Python environment based on the method described by Schmid [20]. In this approach, the dynamic system data is treated as a system of ordinary differential equations, which inherently contains non-linear relations in the spatial and temporal dimensions. The DMD approach subsequently reconstructs locally linear approximations for the spatiotemporal data. Spectral mode shapes and their corresponding frequencies were obtained. The extracted data were then visualized to interpret interactions between the flow structures existing in different regions of surfaces.

4. Overview of hybrid RANS/LES data

The hybrid RANS/LES computations were run with a time step size of 5 μ s using the SA-DDES model for different incidence angles. In each of these simulations, the total simulation time was at least 62.5 ms, which corresponds to 35 flow passes over the length of the airframe. The number of inner iterations was 5 per time step, where the CFL limit was set to 20.

The computations were performed for incidence angles 10°, 11°, 12°, 13°, 14°, 15°, 16° and 17.5°. For each case, the transient response of the rolling moment coefficient (C_l) is converted to the frequency domain using FFT. We observed three different behaviors in the dominant frequencies. In the first level ($10^\circ \leq \sigma \leq 14^\circ$), peak resonant frequency is observed as 900 Hz ($Sr = 0.16$), as seen for, e.g., 12° incidence in Figure 2. As the incidence angle is stepped up to a second level ($15^\circ \leq \sigma \leq 16^\circ$), the resonance peak slightly increases toward 1000 Hz. At this level, a higher-frequency mode starts to appear between 1500-2000 Hz ($0.27 < Sr < 0.36$). Further increase in the incidence angle results in a higher-frequency mode to be dominant, while lower frequency mode also exists in the data.

Figure 2 also shows the FFT of the partial rolling moment data of each wing. It is observed that Wing 3 is the major component undergoing aerodynamic unsteadiness. This fact is apparently a consequence of the flow topology shown by iso-Q-criterion plots representing each incidence level in Figure 3. Wing 3 is exposed to highly turbulent flow conditions due to separations from the forebody wake. One noticeable feature is that the flow structures separated at the end of the nose sphere fluctuate at opposite phases (see Figure 3a-b). These structures transfer turbulent energy to the main wake region for $\sigma < 17^\circ$, while this link does not exist anymore for $\sigma > 17^\circ$, at least by this qualitative inspection. Interestingly, the threshold of this observation corresponds to that of the mode shift in the dominant

frequencies described above. Furthermore, this motivates the author to perform further examination to uncover associated flow interactions through local spectrum analysis.

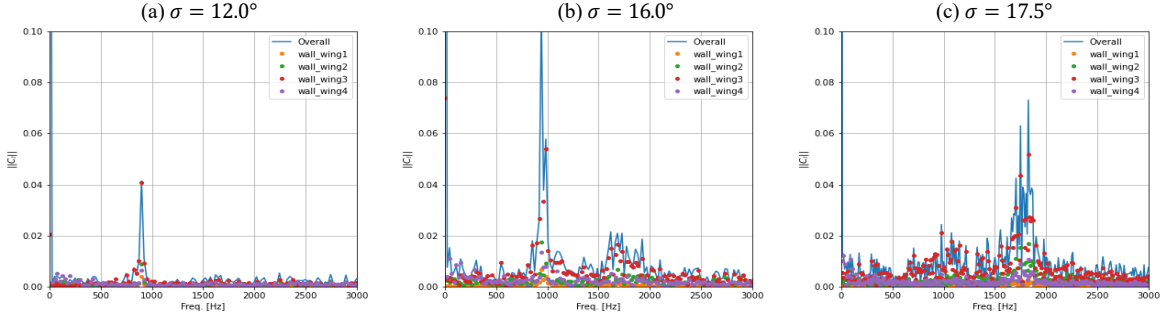


Figure 2. Frequency response of overall and partial C_l data for different incidence angle cases

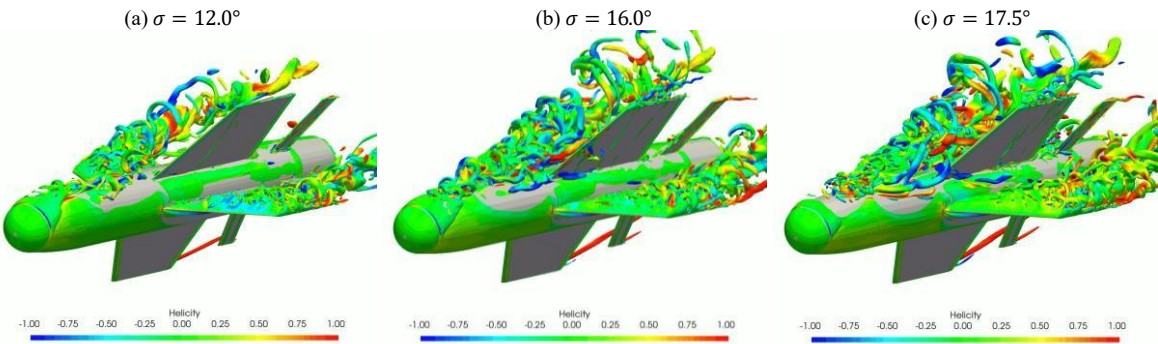


Figure 3. Separated flow topology for different incidence angle cases

5. Local spectrum analysis results

5.1. Wing 3 results

We applied DMD for the spatiotemporal pressure data on Wing 3 for 16- and 17.5-degree incidences. The most dominant modes were extracted for both surfaces. Only the results of the inboard surface (the one facing Wing 4) are presented and discussed here, as the outboard surface has similar harmonic characteristics. The DMD process calculated the temporal mean distribution as the most dominant mode, which is the non-oscillatory mode designated as Mode-0 ($Sr = 0$). The first oscillatory mode (Mode-1) shapes and their associated frequencies are as shown in Figure 4. The dominant frequencies agree with those obtained from FFT analyses. The extracted mode shapes suggest that pressure fluctuations predominantly occur near the leading edge for both cases. The increased incidence angle causes the fluctuating region to get far from the fuselage.

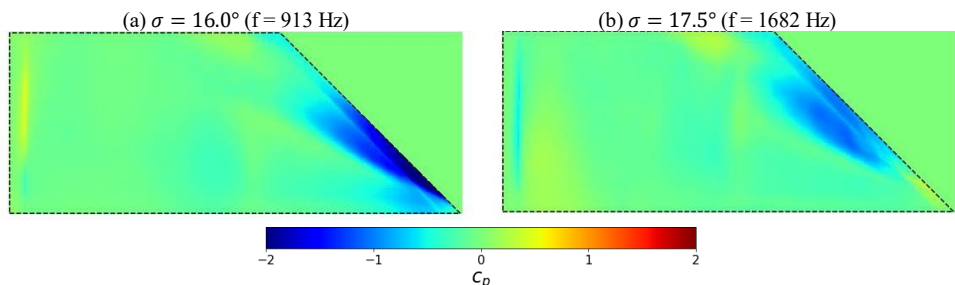


Figure 4. The most dominant oscillatory mode shape over the inboard surface of Wing 3 for different incidence angle cases

The validity of these results depends on how accurately the DMD reconstructed the spatiotemporal data. We adjusted the order of the fit by changing the Singular Value Decomposition (SVD) rank. Too high SVD rank values were avoided since they would lead to overfitting of the data. We reduced the spatial

pressure distribution onto partial C_l contribution of Wing 3 (inboard) surface for both reconstructed (DMD) and original Scale Resolving Simulation (SRS) data. Figure 5 compares those quantities in the time domain. It is shown that the DMD was able to capture primary trends, peak locations, and frequency. Though the model might predict exact amplitudes with an error margin, overall performance was sufficient in terms of the aims of the current study.

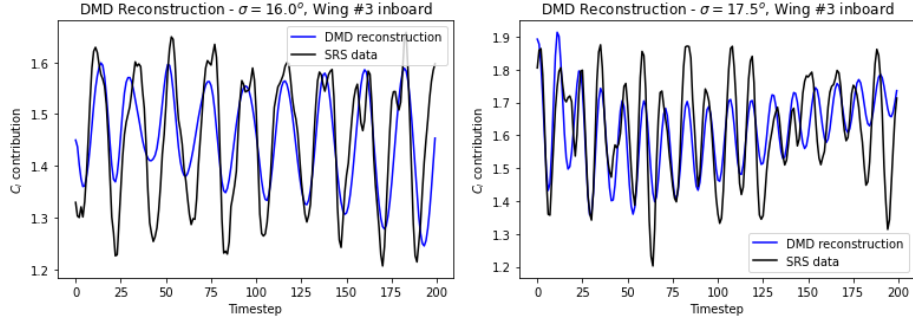


Figure 5. Comparison of reconstructed and original C_l of Wing 3 inboard surface for different incidence angle cases

5.2. Fuselage results

To have a better insight into how body-sourced flow structures affect the Wing 3, we applied the same procedure for the pressure data on fuselage leeward surface for 12-, 16-, and 17.5-degree incidences. Similar to the Wing 3 case, Mode-0 was calculated as the time-averaged distribution. DMD calculated the most dominant harmonic frequencies as 870 Hz, 1010 Hz, and 1720 Hz, respectively. These values are quite comparable to observations on overall C_l . The most dominant oscillatory mode shapes are illustrated in Figure 6, along with the associated frequencies. Wing 3 neighbourhood is observed to have strong fluctuations in these results as well. These fluctuations are found to be harmonic with other oscillatory structures shed from different parts of the upstream body, depending on the incidence angle. For the first two cases, antisymmetric oscillations located at the end of the nose sphere ($x/D = -0.36$) indicate the primary harmonic flow structures. Weaker oscillations located downstream are more distributed, in the 16° case, over the region between nose and Wing3. A much more serious change in the mode shapes is observed while stepping up to 17.5° incidence. In this case, antisymmetric oscillations are emerging from a region much closer to the wing leading edge.

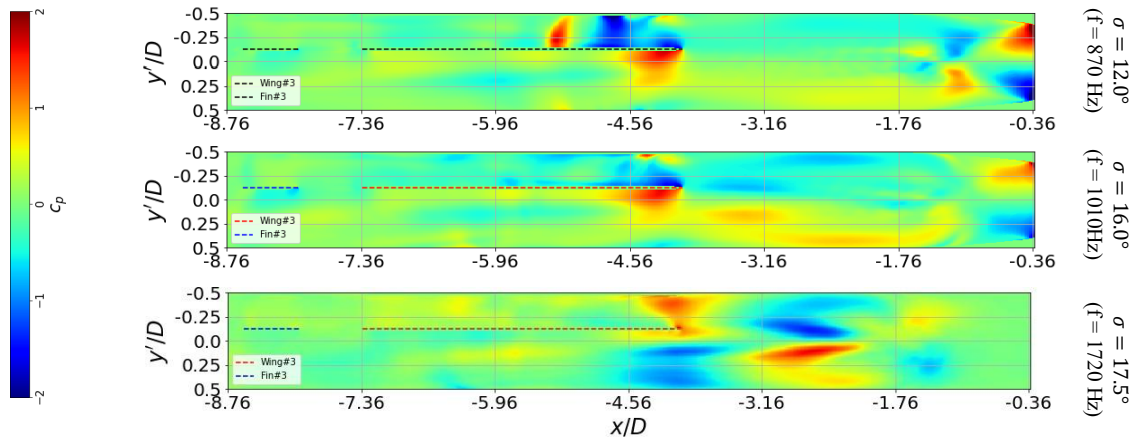


Figure 6. The most dominant oscillatory mode shape over the body leeward surface for different incidence angle cases (nose located at origin)

6. Conclusion

The DMD method is utilized to extract and interpret the harmonic flow features observed after a series of external flow hybrid RANS/LES analyses over a generic body-wing-tail airframe. A spatiotemporal dataset, which is the natural output of such analyses, was processed using the PyDMD library to enhance

the understanding of complex flow physics and to ease the interpretation of flow structures and their interactions. The DMD technique provided spectral content predictions, which are distributed to airframe surface components. Reconstruction models were successful in predicting the most dominant oscillatory mode and its frequency as per comparisons with FFT applied on integrated data.

Vortex-surface interactions play an important role in the characterization of the unsteady aerodynamic features of the specific test problem examined in the current study. By taking advantage of dimensionality reduction, we were able to find out that vortices are shed from the nose at approximately 900 Hz and those shed from the straight part of the forebody at approximately 1700 Hz. The harmonic character shift between 16-17.5 degree incidence angles was also captured. Investigation of potential flow interactions through other components, e.g., side wings, is addressed as future work.

Acknowledgments

The author would like to thank the fellow participants of the NATO STO AVT-390 research group for their collaboration and insightful discussions during the panel group activity. Additional appreciation is expressed to Christian Schnepf (DLR) for sharing the common LK6E2 computational mesh, which was used to generate unsteady flow data in the current study.

References

- [1] 'Vortex Interaction Effects Relevant to Military Air Vehicle Performance', Final Report of Task Group AVT-316, NATO STO Technical Report, STO-TR-AVT-316, 2024
- [2] J. DeSpirito, M.H. Tormalm, C. Schnepf, G.J. Loupy, E. Dikbaş and I.S. Cesur 'Comparisons of predicted and measured aerodynamic characteristics of the DLR LK6E2 missile airframe (scale-resolving)', AIAA 2022-2308, AIAA SciTech 2022 Forum, January 2022. DOI:[10.2514/6.2022-2308](https://doi.org/10.2514/6.2022-2308)
- [3] M.H. Tormalm, J. DeSpirito, C. Schnepf, E. Dikbaş, M. Anderson 'Further comparisons of predicted and measured aerodynamic characteristics of the DLR LK6E2 missile airframe (scale-resolving)', AIAA 2024-4240, AIAA Aviation Forum and Ascend 2024, July 2024, DOI:[10.2514/6.2024-4240](https://doi.org/10.2514/6.2024-4240)
- [4] C. Schnepf, E. Schülein, S. Weiss, U. Henne 'Additional wind tunnel data for the transonic LK6E2 missile airframe', AIAA 2024-4238, AIAA Aviation Forum and Ascend 2024, July 2024, DOI:[10.2514/6.2024-4238](https://doi.org/10.2514/6.2024-4238)
- [5] M. Anderson, C. Schnepf, E. Dikbaş, M.H. Tormalm, J. DeSpirito, G. Loupy, A. Rausa 'Further comparisons of predicted and measured aerodynamic characteristics of the DLR LK6E2 missile airframe (RANS)', AIAA 2024-4239, AIAA Aviation Forum and Ascend 2024, July 2024, DOI:[10.2514/6.2024-4239](https://doi.org/10.2514/6.2024-4239)
- [6] D.J. Lucia, P.S. Beran, W.A. Silva 'Reduced-order modeling: new approaches for computational physics', Prog Aerosp Sci., 2004, DOI:[10.1016/j.paerosci.2003.12.001](https://doi.org/10.1016/j.paerosci.2003.12.001)
- [7] J. Kou, W. Zhang 'Data-driven modeling for unsteady aerodynamics and aeroelasticity', Prog Aerosp Sci, 2021, DOI:[10.1016/j.paerosci.2021.100725](https://doi.org/10.1016/j.paerosci.2021.100725)
- [8] Y. Long, X. Guo, T. Xiao 'Research, Application and Future Prospect of Mode Decomposition in Fluid Mechanics', Aerosp., 2024, DOI:[10.3390/sym16020155](https://doi.org/10.3390/sym16020155)
- [9] J.A. Morínigo, P. Anaya-Ruiz, A. Bustos, R. Mayo-Garcia 'Unsteady RANS-based DMD analysis of airfoil NACA0015 with Gurney flap', Int J Heat Fluid Flow, 2023, DOI:[10.1016/j.ijheatfluidflow.2022.109099](https://doi.org/10.1016/j.ijheatfluidflow.2022.109099)
- [10] W. Mallik, D.E. Ravet 'Aerodynamic damping investigations of light dynamic stall on a pitching airfoil via modal analysis', J Fluids Struc, 2020, DOI:[10.1016/j.jfluidstructs.2020.103111](https://doi.org/10.1016/j.jfluidstructs.2020.103111)
- [11] F. Qu, T. Wang, C. Liu, J. Fu, J. Bai 'Aerodynamic shape optimization of the vortex-shock integrated waverider over a wide speed range', Aerosp Sci Tech, 2023, DOI:[10.1016/j.ast.2023.108696](https://doi.org/10.1016/j.ast.2023.108696)
- [12] Y. Zhang, L. Zhang, X. Deng, H. Sun 'POD and DMD analysis of complex separation flows over an aircraft model at high angle of attack', Physics of Gases, 2018, DOI:[10.19527/j.cnki.2096-1642.2018.05.004](https://doi.org/10.19527/j.cnki.2096-1642.2018.05.004)
- [13] B.F. Ma, S.L. Yin 'Vortex oscillations around a hemisphere-cylinder body with a high fineness ratio', AIAA J, 2018, DOI: [10.2514/1.J056047](https://doi.org/10.2514/1.J056047)
- [14] E.A. Luke 'A rule-based specification system for computational fluid dynamics', PhD thesis, Mississippi State University, USA, 1999
- [15] E.A. Luke, X. Tong, R. Chamberlein 'flowPsi source code, version 1-0-p4', 2021
- [16] P.R. Spalart, S.R. Allmaras 'A one-equation turbulence model for aerodynamic flows', Recherche Aerospatiale, 1994, No. 1, pp. 5-21
- [17] P.R. Spalart, S. Deck, M.L. Shur, K.D. Squires, M.K. Strelets, A. Travin 'A new version of Detached-Eddy Simulation, resistant to ambiguous grid densities', Theoret. Comput. Fluid Dynamics, 2006, DOI:[10.1007/s00162-006-0015-0](https://doi.org/10.1007/s00162-006-0015-0)
- [18] N. Ahmed, K.R. Rao 'Fast Fourier Transform' book chapter pp 54-84, Orthogonal Transforms for Digital Signal Processing, Springer, 1975; DOI:[10.1007/978-3-642-45450-9_4](https://doi.org/10.1007/978-3-642-45450-9_4)
- [19] N. Demo, M. Tezzele, G. Rozza 'PyDMD: Python dynamic mode decomposition', J Open Source Software, 2018, DOI:[10.21105/joss.00530](https://doi.org/10.21105/joss.00530)
- [20] P.J. Schmid 'Dynamic Mode Decomposition of numerical and experimental data', J Fluid Mech, 2010, DOI:[10.1017/S0022112010001217](https://doi.org/10.1017/S0022112010001217)